Scattering-matrix formalism of electron transport through three-terminal quantum structures: formulation and application to Y-junction devices

2002 J. Phys.: Condens. Matter 14 12513

(http://iopscience.iop.org/0953-8984/14/47/324)

INSTITUTE OF PHYSICS PUBLISHING JOURNAL OF PHYSICS: CONDENSED MATTER

J. Phys.: Condens. Matter **14** (2002) 12513–12528 PII: S0953-8984(02)39328-7

Scattering-matrix formalism of electron transport through three-terminal quantum structures: formulation and application to Y-junction devices

Dan Csontos and H Q Xu

Solid State Physics, Lund University, PO Box 118, SE-221 00 Lund, Sweden

E-mail: dan.csontos@ftf.lth.se and hongqi.xu@ftf.lth.se

Received 10 July 2002
Published 15 November 2002
Online at stacks.iop.org/JPhysCM/14/12513

Abstract

In this paper we present a formalism for the calculation of electron transport through three-terminal junction devices, which have received attention due to their recently demonstrated non-linear electrical properties. The formalism, which is based on the scattering-matrix method, takes quantum interference effects fully into account. Furthermore, the formalism provides numerical stability in the calculations as well as large flexibility in the modelling of arbitrary potential profiles due to the common basis approach used in the formulation. The method is used to calculate the transport properties for Y-shaped three-terminal ballistic junction (TBJ) structures with configurations typical of recently performed experiments. Quantum interference effects are shown to strongly influence the transport characteristics of TBJ structures due to complex scattering of the electrons in the cavity-like coupling window between the three arms of the device. The theoretical approach presented in this paper provides a flexible tool for the study of such quantum interference effects, which may play an important role in the design and functionality of future nanoscale devices based on three-terminal junctions.

1. Introduction

Three-terminal junctions have very recently emerged as excellent candidates for use as building blocks in the formation of nanoscale electronic devices. On one hand, rapid development in the field of carbon nanotubes [1–3] has enabled the realization of carbon nanotube Y junctions [4–7] which have displayed interesting nonlinear electric properties [5, 6]. The implementation of carbon nanotubes in real electronic devices is, however, still difficult due to the lack of technologies for controlled production of such junctions and for individually contacting the three arms. On the other hand, three-terminal ballistic junction (TBJ) devices based on high-quality semiconductor heterostructures have been realized with state of the art nanofabrication

technology [8–11]. Originally, Y-branch switches (Y-shaped TBJ devices) were proposed with the aim of realizing low switching voltages in a single-mode, coherent regime of operation [12–14]. In such a device, electrons injected from a source contact are deflected by a lateral electric field, created by gates in the branching region, into either of two drain contacts.

A different type of operation for three-terminal junction devices was recently theoretically investigated by Xu [15, 16], who also predicted new, exploitable non-linear transport phenomena based on the ballistic nature of the electron transport. According to these predictions, when finite voltages V_L and V_R are applied to the left and right arms of a symmetric Y junction device in push–pull fashion, i.e., with $V_L = -V_R$, the voltage at the central branch will always be negative. It was also predicted that these properties are inherent to TBJ devices in general. These findings were recently verified experimentally in InGaAs/InP [8] and AlGaAs/GaAs [9] Y-shaped TBJs as well as InGaAs/InP T-shaped TBJs [10]. In the latter case, room-temperature operation was also demonstrated. It is interesting to note that similar effects have also been predicted for carbon nanotube Y junctions [17, 18].

The properties found for TBJs are potentially important for a number of future electronic applications on the nanometre scale. For example, it has been proposed [15] that TBJs operating in the push–pull fashion discussed above can have rectifying properties due to the negative output voltage at the central branch. Other proposed applications include second-harmonic generation [15, 19] and the use of TBJs as diodes and triodes [16], as well as logic gates [15, 19]. Some of these devices have already been realized experimentally based on high-quality semiconductor heterostructures [11]. In addition, these devices can be made from semiconductor heterostructures with a one-step lithography process and, thus, the nanoimprint lithography technique can be exploited to achieve mass production of these devices [20].

The theoretical predictions and analyses given in [15] were made under the assumption that the three-terminal junction can be modelled by connecting three quantum point contacts via a ballistic cavity with adiabatic boundaries, thus neglecting backscattering of electrons. The question is to what extent quantum interference effects, which are expected to be of importance for waveguide devices on the nanometre scale [21–29], influence the electron transport through TBJs. Complex scatterings and formation of quasi-bound states in the central junction region of the TBJ may strongly influence the properties of the electron transport. Several investigations of the two-terminal electron transport through electron waveguides (quantum wires) coupled via some ballistic cavity have shown strong signatures of interference effects arising from the scattering of electron waves between the wires and the cavity [26–29]. Similar effects are therefore expected to be importance for electron transport through TBJs, where the central connecting region forms an electron cavity. Furthermore, electron waves may be scattered in the TBJ due to impurities [30], boundary roughness [31], differences in the density of states of the three branches resulting from intentional or un-intentional asymmetries in the TBJ etc. These scattering mechanisms are important for the understanding of the underlying physics as well as the properties and functionalities relevant to applications using TBJs. However, to the best of our knowledge, no extensive studies of electron transport through TBJs have been performed to this day. The few theoretical studies that have been carried out [12–15] have only treated simple cases, using theoretical models unsuitable for fully taking into account scattering in the devices. It is the purpose of this paper to derive an adequate formalism for the calculation of electron transport in TBJs, taking into consideration the above-mentioned scattering mechanisms.

In the past few years, several theoretical and numerical methods, such as the transfer-matrix method [32, 33], the time-dependent approach [34], the recursive Green function method [35, 36] and the scattering-matrix method [37–40], have been used for the study of electron transport in quantum waveguides with different configurations. In particular, the

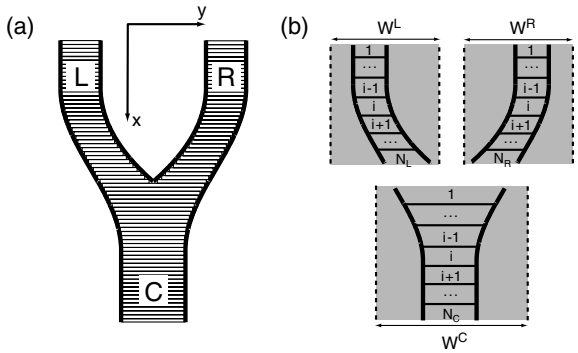

Figure 1. (a) Schematics of a Y-junction device. The hatched region illustrates the domain in which electron transport is allowed. (b) Modelling of the potential profile is done by dividing the structure into a number of segments. These segments are made small enough such that in each segment the potential profile may be assumed to be of transverse dependence only. Within each branch, a basis set is used in the calculation of the transverse modes in each of the segments. The basis sets are eigensolutions to an infinite-square-well problem. Shaded regions illustrate infinite-square-well potentials (zero potential in shaded regions) in which the basis sets are defined.

scattering-matrix method is well established and has the advantage of being numerically stable and of providing the possibility of treating complicated two-dimensional potential profiles which are hard to investigate using lattice-based models. In addition, evanescent states are naturally included in the analysis without causing numerical instabilities, even when applied to strongly modulated structures, see e.g. [37, 38]. This method has been successfully tested and used in recent years for the study of a variety of systems including e.g. disordered quantum wires [30, 31], antidot arrays [37], disordered Aharonov–Bohm interferometers [39], quantum dot structures [40–43], quantum coherent networks [44], coupled quantum wires [45] etc. The method has, as far as we know, not been used for studies of electron transport in three-terminal structures, and a formulation and implementation of the method has not yet been demonstrated.

In this paper we develop a scattering-matrix formalism based on a common basis approach for the calculation of electron transport in a Y-shaped three-terminal junction. The common basis approach allows for large flexibility in the choice of lateral and longitudinal potential profiles, including impurities and boundary roughness as well as arbitrary potential profiles both along and perpendicular to the direction of transport. We will show how the formalism may be implemented and used for the study of realistic Y-junction structures, and exemplify the use by calculating the transport properties of TBJs with geometrical configurations typical to experiments.

The paper is organized as follows. In section 2 we give a derivation of the formalism and discuss some numerical issues. Section 3 is devoted to the implementation and use of the method in practical calculations. Finally, a brief summary and some remarks are given.

2. Formalism

Consider the schematics of the Y-shaped three-terminal junction shown in figure 1. The left, right and central branches (arms), which are labelled by L, R, C, are each divided into a large number of small segments, which are small enough such that the potential profile in each segment is of transverse dependence only. In each segment, here labelled i, the motion of an electron with a given energy ε is described by a wavefunction satisfying the following

effective-mass Schrödinger equation:

$$\left[-\frac{\hbar^2}{2m^*}\left(\frac{\partial^2}{\partial x^2}+\frac{\partial^2}{\partial y^2}\right)+U_c^{b,i}(y)+U_s^{b,i}(y)\right]\Psi^{b,i}(x,y)=\varepsilon\Psi^{b,i}(x,y), \tag{1}$$

where $b = L, R, C$ labels the three branches, $U_c^{b,i}(y)$ describes the transverse confinement defined by the boundaries of the three-terminal junction (solid line in figure 1(b)), $U_s^{b,i}(y)$ is the transverse potential inside segment i of branch b and m^* is the effective mass of the electron.

Expanding the wavefunction $\Psi^{b,i}(x, y)$ in terms of the transverse modes $\{\phi_n^{b,i}(y)\}$, with eigenvalues $\{E_n^{b,i}\}$, of segment i in branch b, and the free electron wavefunction describing the motion in the direction of transport, yields the relation

$$\Psi^{b,i}(x,y)=\sum_n[a_n^{b,i+}\mathrm{e}^{\mathrm{i}k_n^{b,i}(x-x_0^{b,i})}+a_n^{b,i-}\mathrm{e}^{-\mathrm{i}k_n^{b,i}(x-x_0^{b,i})}]\phi_n^{b,i}(y), \tag{2}$$

where $x_0^{b,i}$ is a reference coordinate along the x direction of segment i, and $k_n^{b,i} = [2m^*(\varepsilon - E_n^{b,i})/\hbar^2]^{1/2}$ are longitudinal wavenumbers which may be either real or imaginary, thus corresponding to propagating or evanescent states, respectively. The labels $+(-)$ denote states that are propagating forwards or evanescent (propagating backwards or exponentially increasing). The transverse wavefunctions $\{\phi_n^{b,i}(y)\}$ satisfy the equation

$$\left[-\frac{\hbar^2}{2m^*}\frac{\mathrm{d}^2}{\mathrm{d}y^2}+U_c^{b,i}(y)+U_s^{b,i}(y)\right]\phi_n^{b,i}(y)=E_n^{b,i}\phi_n^{b,i}(y). \tag{3}$$

In order to find the unknown transverse eigenmodes $\{\phi_n^{b,i}(y)\}$ we perform an expansion in terms of the complete basis sets [37] $\{\psi_\alpha^b(y)\}$ (one common basis set for each branch), which are chosen to be eigensolutions of the infinite-square-well potential problem. The basis sets are defined within the widths W^b as shown in figure 1(b), and thus have the form

$$\psi_\alpha^b(y)=\sqrt{\frac{2}{W^b}}\sin[\alpha\pi(y-y_0^b)/W^b] \qquad \alpha=1,2,3,\ldots, \tag{4}$$

where y_0^b and $y_0^b + W^b$ are the transverse boundaries of the infinite-square-well potential. The wavefunction $\Psi^{b,i}(x, y)$ may thus be written according to

$$\Psi^{b,i}(x,y)=\sum_\alpha\psi_\alpha^b(y)\sum_n d_{\alpha n}^{b,i}[a_n^{b,i+}\mathrm{e}^{\mathrm{i}k_n^{b,i}(x-x_0^{b,i})}+a_n^{b,i-}\mathrm{e}^{-\mathrm{i}k_n^{b,i}(x-x_0^{b,i})}]. \tag{5}$$

By inserting equation (5) into the Schrödinger equation (1), multiplying by $\psi_\beta^b(y)$ and integrating with respect to y, we obtain the following system of equations, which renders the transverse eigenmodes $\phi_n^{b,i}(y)$ and the corresponding eigenvalues $E_n^{b,i}$, as well as the expansion coefficients $d_{\alpha n}^{b,i}$:

$$\sum_\alpha[(\epsilon_\beta^b-E_n^{b,i})\delta_{\beta\alpha}+\langle\psi_\beta^b(y)|U_c^{b,i}(y)+U_s^{b,i}(y)|\psi_\alpha^b(y)\rangle]d_{\alpha n}^{b,i}=0, \qquad \beta=1,2,3,\ldots, \tag{6}$$

where the terms ϵ_β^b are eigenenergies to the corresponding basis functions $\psi_\beta^b(y)$.

The unknowns remaining to be found are the coefficients $\{a_n^{b,i\pm}\}$ in equation (5). These coefficients may be obtained by means of mode-matching techniques. For a two-terminal system (such as each individual branch in figure 1(b)), one can relate the coefficients in two adjacent segments i and $j = i + 1$ by a (two-terminal) transfer matrix $\boldsymbol{T}^b(i, j)$ according to

$$\begin{pmatrix}\boldsymbol{A}^{b,i+}\\ \boldsymbol{A}^{b,i-}\end{pmatrix}=\boldsymbol{T}^b(i,j)\begin{pmatrix}\boldsymbol{A}^{b,j+}\\ \boldsymbol{A}^{b,j-}\end{pmatrix}, \tag{7}$$

where $\boldsymbol{A}^{b,i\pm}$ are column vectors containing the coefficients $\{a_n^{b,i\pm}\}$. In contrast, in the scattering-matrix method the coefficients in two adjacent segments i and $j = i + 1$ are related by a (two-terminal) scattering-matrix according to

$$\begin{pmatrix} \boldsymbol{A}^{b,j+} \\ \boldsymbol{A}^{b,i-} \end{pmatrix} = \boldsymbol{S}^b(i, j) \begin{pmatrix} \boldsymbol{A}^{b,i+} \\ \boldsymbol{A}^{b,j-} \end{pmatrix}, \tag{8}$$

thus separating the incoming states from the outgoing states.

It has been previously shown [37] that

(i) the total scattering matrix $\boldsymbol{S}^b(1, N)$ (of a two-terminal system containing N segments) connecting the amplitudes of the states in the outmost segments of the structure may be calculated iteratively provided that $\boldsymbol{S}^b(1, 2)$ is known,
(ii) the scattering matrix $\boldsymbol{S}^b(1, i + 1)$ connecting the amplitudes in the first segment of the two-terminal system to the ones in an arbitrary segment $i + 1$ may be obtained in terms of the scattering and transfer matrices, $\boldsymbol{S}^b(1, i)$ and $\boldsymbol{T}^b(i, i + 1)$, and
(iii) the submatrices of $\boldsymbol{S}^b(1, i + 1)$ are given by ($j = i + 1$ and labels b omitted for brevity)

$$\begin{aligned}
\boldsymbol{S}_{11}(1, j) &= [\mathbf{1} - \boldsymbol{T}_{11}^{-1}(i, j)\boldsymbol{S}_{12}(1, i)\boldsymbol{T}_{21}(i, j)]^{-1}\boldsymbol{T}_{11}^{-1}(i, j)\boldsymbol{S}_{11}(1, i) \\
\boldsymbol{S}_{12}(1, j) &= [\mathbf{1} - \boldsymbol{T}_{11}^{-1}(i, j)\boldsymbol{S}_{12}(1, i)\boldsymbol{T}_{21}(i, j)]^{-1} \\
&\quad \times [\boldsymbol{T}_{11}^{-1}(i, j)\boldsymbol{S}_{12}(1, i)\boldsymbol{T}_{22}(i, j) - \boldsymbol{T}_{11}^{-1}(i, j)\boldsymbol{T}_{12}(i, j)] \\
\boldsymbol{S}_{21}(1, j) &= \boldsymbol{S}_{21}(1, i) + \boldsymbol{S}_{22}(1, i)\boldsymbol{T}_{21}(i, j)\boldsymbol{S}_{11}(1, j) \\
\boldsymbol{S}_{22}(1, j) &= \boldsymbol{S}_{22}(1, i)\boldsymbol{T}_{21}(i, j)\boldsymbol{S}_{12}(1, j) + \boldsymbol{S}_{22}(1, i)\boldsymbol{T}_{22}(i, j).
\end{aligned} \tag{9}$$

The transfer matrix $\boldsymbol{T}^b(i, j)$ is obtained [23, 46, 47] by imposing the conditions of continuity of the wavefunctions, $\Psi^{b,i}(x, y)$ and $\Psi^{b,i+1}(x, y)$, and of their derivatives at interfaces between adjacent segments, and has the form

$$\boldsymbol{T}^b(i, j) = \begin{bmatrix} \gamma^{b,i} & 0 \\ 0 & (\gamma^{b,i})^{-1} \end{bmatrix}^{-1} \begin{pmatrix} \boldsymbol{D}^{b,i} & \boldsymbol{D}^{b,i} \\ \boldsymbol{D}^{b,i}\boldsymbol{K}^{b,i} & -\boldsymbol{D}^{b,i}\boldsymbol{K}^{b,i} \end{pmatrix}^{-1} \begin{pmatrix} \boldsymbol{D}^{b,j} & \boldsymbol{D}^{b,j} \\ \boldsymbol{D}^{b,j}\boldsymbol{K}^{b,j} & -\boldsymbol{D}^{b,j}\boldsymbol{K}^{b,j} \end{pmatrix} \tag{10}$$

where the submatrices $\gamma^{b,i}$, $\boldsymbol{D}^{b,i}$ and $\boldsymbol{K}^{b,i}$ are given by

$$(\gamma^{b,i})_{nn} = \mathrm{e}^{\mathrm{i}k_n^{b,i}l^{b,i}}, \qquad (\boldsymbol{D}^{b,i})_{\alpha n} = d_{\alpha n}^{b,i}, \qquad (\boldsymbol{K}^{b,i})_{nn} = k_n^{b,i}, \tag{11}$$

and $l^{b,i}$ is the longitudinal size of segment i.

Thus, (two-terminal) scattering matrices of the form $\boldsymbol{S}^b(1, i + 1)$ may be calculated iteratively using equations (9), (10), provided the scattering matrix $\boldsymbol{S}^b(1, 2)$ is known, rendering the successive evaluation of $\boldsymbol{S}^b(1, 3)$, $\boldsymbol{S}^b(1, 4)$, ..., $\boldsymbol{S}^b(1, N)$. The explicit form of $\boldsymbol{S}^b(1, 2)$ is given in appendix A.

In our model we separate the motion in the left and right branches and use the two-terminal scattering-matrix formalism above in order to establish a relation between the amplitudes of the states in the outmost segments of the left and right branches and thus (assuming $N_L(N_R)$ segments for the left(right) branch)

$$\begin{aligned}
\begin{pmatrix} \boldsymbol{A}^{L,N_L+} \\ \boldsymbol{A}^{L,1-} \end{pmatrix} &= \boldsymbol{S}^L(1, N_L) \begin{pmatrix} \boldsymbol{A}^{L,1+} \\ \boldsymbol{A}^{L,N_L-} \end{pmatrix} \\
\begin{pmatrix} \boldsymbol{A}^{R,N_R+} \\ \boldsymbol{A}^{R,1-} \end{pmatrix} &= \boldsymbol{S}^R(1, N_R) \begin{pmatrix} \boldsymbol{A}^{R,1+} \\ \boldsymbol{A}^{R,N_R-} \end{pmatrix}.
\end{aligned} \tag{12}$$

In order to calculate the transport properties of a three-terminal device of the type depicted in figure 1 we wish to calculate the amplitudes $\boldsymbol{A}^{L,1\pm}$, $\boldsymbol{A}^{R,1\pm}$ and $\boldsymbol{A}^{C,N_C\pm}$, of the states in the

outmost segments of the system. Similarly to the approach discussed above, we can relate these amplitudes by a three-terminal scattering matrix, $\boldsymbol{S}'(LR, N_C)$, which, using the notations above, satisfies the following relation:

$$\begin{pmatrix} \boldsymbol{A}^{C,N_C+} \\ \boldsymbol{A}^{R,1-} \\ \boldsymbol{A}^{L,1-} \end{pmatrix} = \boldsymbol{S}'(LR, N_C) \begin{pmatrix} \boldsymbol{A}^{R,1+} \\ \boldsymbol{A}^{L,1+} \\ \boldsymbol{A}^{C,N_C-} \end{pmatrix}. \tag{13}$$

We proceed to derive an expression for $\boldsymbol{S}'(LR, 1)$, which connects the amplitudes of the states in the first segments of the left and right branches and the first segment of the central branch (see figure 1(b) for definitions). Subsequently, we show an iterative relation, analogous to equation (9), for the three-terminal scattering matrix, $\boldsymbol{S}'(LR, j = i + 1)$, which enables the calculation of the total scattering matrix of the system, $\boldsymbol{S}'(LR, N_C)$.

First, the connection between the wavefunctions in the left, right and central branches at the interface at $x = x_0^{C,1}$ is obtained by imposing the conditions of continuity of the wavefunctions, Ψ^{L,N_L}, Ψ^{R,N_R} and $\Psi^{C,1}$, and of their first derivatives at the corresponding interface. Thus, we need to consider the following set of equations:

$$\Psi^{L,N_L}(x_0^{C,1}, y) + \Psi^{R,N_R}(x_0^{C,1}, y) = \Psi^{C,1}(x_0^{C,1}, y) \tag{14a}$$

$$\frac{\partial}{\partial x}\left[\Psi^{L,N_L}(x, y) + \Psi^{R,N_R}(x, y)\right]_{x=x_0^{C,1}} = \frac{\partial}{\partial x}[\Psi^{C,1}(x, y)]_{x=x_0^{C,1}}, \tag{14b}$$

where the wavefunctions $\Psi^{b,i}$ have the form stated in equation (5).

In order to eliminate the remaining position dependence (y) in equations (14a) and (14b), we multiply both sides of the equations with basis functions $\psi_\beta^b(y)$ corresponding to one of the three basis sets used in the wavefunction expansion of equation (5) and subsequently integrate with respect to y. The basis sets $\{\psi_\beta^L(y)\}$ and $\{\psi_\beta^R(y)\}$ are spatially separated and defined within $y_0^L \leqslant y \leqslant y_0^L + W^L$ and $y_0^R \leqslant y \leqslant y_0^R + W^R$, respectively. In our model we further assume that these two regions are defined within $y_0^C \leqslant y \leqslant y_0^C + W^C$ (see figure 2 for schematics). Using this assumption, equation (14a) should be multiplied by $\psi_\beta^C(y)$ and integrated with respect to y. Equation (14b) on the other hand should be multiplied in turn by $\psi_\beta^L(y)$ and $\psi_\beta^R(y)$ and be integrated with respect to y. The resulting relation can be written in the matrix form

$$\boldsymbol{M}_L \boldsymbol{M}_\gamma \begin{pmatrix} \boldsymbol{A}^{R,N_R+} \\ \boldsymbol{A}^{L,N_L+} \\ \boldsymbol{A}^{R,N_R-} \\ \boldsymbol{A}^{L,N_L-} \end{pmatrix} = \boldsymbol{M}_R \begin{pmatrix} \boldsymbol{A}^{C,1+} \\ \boldsymbol{A}^{C,1-} \end{pmatrix}, \tag{15}$$

with

$$\boldsymbol{M}_L = \begin{pmatrix} \boldsymbol{F}^R\boldsymbol{D}^{R,N_R} & \boldsymbol{F}^L\boldsymbol{D}^{L,N_L} & \boldsymbol{F}^R\boldsymbol{D}^{R,N_R} & \boldsymbol{F}^L\boldsymbol{D}^{L,N_L} \\ \boldsymbol{D}^{R,N_R}\boldsymbol{K}^{R,N_R} & 0 & -\boldsymbol{D}^{R,N_R}\boldsymbol{K}^{R,N_R} & 0 \\ 0 & \boldsymbol{D}^{L,N_L}\boldsymbol{K}^{L,N_L} & 0 & -\boldsymbol{D}^{L,N_L}\boldsymbol{K}^{L,N_L} \end{pmatrix}$$

$$\boldsymbol{M}_\gamma = \begin{pmatrix} \gamma^{R,N_R} & 0 & 0 & 0 \\ 0 & \gamma^{L,N_L} & 0 & 0 \\ 0 & 0 & (\gamma^{R,N_R})^{-1} & 0 \\ 0 & 0 & 0 & (\gamma^{L,N_L})^{-1} \end{pmatrix} \tag{16}$$

$$\boldsymbol{M}_R = \begin{bmatrix} \boldsymbol{D}^{C,1} & \boldsymbol{D}^{C,1} \\ (\boldsymbol{F}^R)^T\boldsymbol{D}^{C,1}\boldsymbol{K}^{C,1} & -(\boldsymbol{F}^R)^T\boldsymbol{D}^{C,1}\boldsymbol{K}^{C,1} \\ (\boldsymbol{F}^L)^T\boldsymbol{D}^{C,1}\boldsymbol{K}^{C,1} & -(\boldsymbol{F}^L)^T\boldsymbol{D}^{C,1}\boldsymbol{K}^{C,1} \end{bmatrix},$$

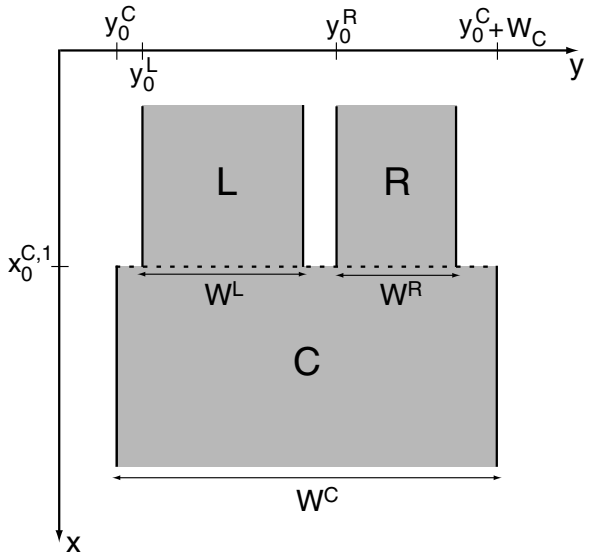

Figure 2. Schematic view of the regions in the left, right and central branches of a Y-junction in which the complete basis sets used in the calculations are defined (shaded regions). The approach is based on the assumption that the basis sets in the left and right branches are defined within $y_0^C \leqslant y \leqslant y_0^C + W^C$.

where $\boldsymbol{D}^{b,i}$, $\boldsymbol{\gamma}^{b,i}$ and $\boldsymbol{K}^{b,i}$ are matrices with elements given by equation (11) and $\boldsymbol{F}^L$ and $\boldsymbol{F}^R$ are matrices containing overlap integrals of the form

$$(\boldsymbol{F}^R)_{\beta\alpha} = \int_{y_0^R}^{y_0^R+W^R} \psi_\beta^C(y)\psi_\alpha^R(y)\,\mathrm{d}y$$
$$(\boldsymbol{F}^L)_{\beta\alpha} = \int_{y_0^L}^{y_0^L+W^L} \psi_\beta^C(y)\psi_\alpha^L(y)\,\mathrm{d}y. \tag{17}$$

The dimensions of the matrices in the equations above are determined by the numbers of basis functions, M_L, M_R and M_C, used in the wavefunction expansions of equation (5). In principle, M_L, M_R and M_C should go to infinity. In practice, however, equation (6) has to be solved numerically by truncating M_L, M_R, M_C at high transverse levels. To proceed we also assume $M_C = M_L + M_R$.

Using the results of equation (12) we can eliminate the coefficient vectors $\boldsymbol{A}^{L,N_L}$ and $\boldsymbol{A}^{R,N_R}$ in equation (15) and obtain the following relation:

$$\begin{pmatrix} \boldsymbol{A}^{C,1+} \\ \boldsymbol{A}^{R,1-} \\ \boldsymbol{A}^{L,1-} \end{pmatrix} = \boldsymbol{S}'(LR,1) \begin{pmatrix} \boldsymbol{A}^{R,1+} \\ \boldsymbol{A}^{L,1+} \\ \boldsymbol{A}^{C,1-} \end{pmatrix}. \tag{18}$$

The three-terminal scattering matrix $\boldsymbol{S}'(LR,1)$ can be written in terms of four $M_C \times M_C$ block matrices according to (for derivation of $\boldsymbol{S}'(LR,1)$ see appendix B):

$$\begin{aligned}
\boldsymbol{S}'_{11}(LR,1) &= 2[\mathbf{1} + (\boldsymbol{D}^{C,1})^{-1}\boldsymbol{P}\boldsymbol{Q}^{-1}\boldsymbol{R}]^{-1}(\boldsymbol{D}^{C,1})^{-1}\boldsymbol{P}\boldsymbol{\Gamma}[\mathbf{1} - \boldsymbol{S}_{12}\boldsymbol{\Gamma}\boldsymbol{W}\boldsymbol{\Gamma}]^{-1}\boldsymbol{S}_{11} \\
\boldsymbol{S}'_{12}(LR,1) &= [\mathbf{1} + (\boldsymbol{D}^{C,1})^{-1}\boldsymbol{P}\boldsymbol{Q}^{-1}\boldsymbol{R}]^{-1}\{4(\boldsymbol{D}^{C,1})^{-1}\boldsymbol{P}\boldsymbol{\Gamma}[\mathbf{1} - \boldsymbol{S}_{12}\boldsymbol{\Gamma}\boldsymbol{W}\boldsymbol{\Gamma}]^{-1} \\
&\quad \times \boldsymbol{S}_{12}\boldsymbol{\Gamma}\boldsymbol{U}^{-1}\boldsymbol{Q}^{-1}\boldsymbol{R} - \mathbf{1} + (\boldsymbol{D}^{C,1})^{-1}\boldsymbol{P}\boldsymbol{Q}^{-1}\boldsymbol{R}\} \\
\boldsymbol{S}'_{21}(LR,1) &= \boldsymbol{S}_{21} + \boldsymbol{S}_{22}[\mathbf{1} - \boldsymbol{\Gamma}\boldsymbol{W}\boldsymbol{\Gamma}\boldsymbol{S}_{12}]^{-1}[\boldsymbol{\Gamma}\boldsymbol{W}\boldsymbol{\Gamma}\boldsymbol{S}_{11}] \\
\boldsymbol{S}'_{22}(LR,1) &= 2\boldsymbol{S}_{22}[\mathbf{1} - \boldsymbol{\Gamma}\boldsymbol{W}\boldsymbol{\Gamma}\boldsymbol{S}_{12}]^{-1}\boldsymbol{\Gamma}\boldsymbol{U}^{-1}\boldsymbol{Q}^{-1}\boldsymbol{R},
\end{aligned} \tag{19}$$

where

$$
\begin{aligned}
\boldsymbol{S}_{ij} &= \begin{pmatrix} \boldsymbol{S}_{ij}^{R} & 0 \\ 0 & \boldsymbol{S}_{ij}^{L} \end{pmatrix} \qquad i, j = 1, 2 \\
\boldsymbol{U} &= \mathbf{1} + \boldsymbol{Q}^{-1}\boldsymbol{R}(\boldsymbol{D}^{C,1})^{-1}\boldsymbol{P} \\
\boldsymbol{V} &= \mathbf{1} - \boldsymbol{Q}^{-1}\boldsymbol{R}(\boldsymbol{D}^{C,1})^{-1}\boldsymbol{P} \\
\boldsymbol{W} &= \boldsymbol{U}^{-1}\boldsymbol{V} \\
\boldsymbol{P} &= \begin{pmatrix} \boldsymbol{F}^{R}\boldsymbol{D}^{R,N_R} & \boldsymbol{F}^{L}\boldsymbol{D}^{L,N_L} \end{pmatrix} \\
\boldsymbol{Q} &= \begin{pmatrix} \boldsymbol{D}^{R,N_R}\boldsymbol{K}^{R,N_R} & 0 \\ 0 & \boldsymbol{D}^{L,N_L}\boldsymbol{K}^{L,N_L} \end{pmatrix} \\
\boldsymbol{R} &= \begin{bmatrix} (\boldsymbol{F}^{R})^{T}\boldsymbol{D}^{C,1}\boldsymbol{K}^{C,1} \\ (\boldsymbol{F}^{L})^{T}\boldsymbol{D}^{C,1}\boldsymbol{K}^{C,1} \end{bmatrix} \\
\boldsymbol{\Gamma} &= \begin{bmatrix} \gamma^{R,N_R} & 0 \\ 0 & \gamma^{L,N_L} \end{bmatrix},
\end{aligned}
\tag{20}
$$

are $M_C \times M_C$ matrices. We emphasize that in the derivation of $\boldsymbol{S}'(LR, 1)$ we have avoided any inversions of $\boldsymbol{F}^{L}$ and $\boldsymbol{F}^{R}$. Such inversions can lead to numerical instability[1].

Knowing $\boldsymbol{S}'(LR, 1)$, the only remaining step is to calculate the total scattering matrix, $\boldsymbol{S}'(LR, N_C)$, which connects the amplitudes of the states in the outmost segments of the three-terminal junction (see equation (13)). We use an approach similar to the one used in [37] in the scattering-matrix approach for two-terminal systems. Given a known scattering matrix $\boldsymbol{S}'(LR, i)$, a new scattering matrix $\boldsymbol{S}'(LR, i+1)$ can be calculated using $\boldsymbol{S}'(LR, i)$ and the transfer matrix $\boldsymbol{T}^{C}(i, i+1)$ connecting the amplitudes in the two adjacent segments i and $i+1$ (see equation (10)). Thus, an iterative relation for the scattering matrix $\boldsymbol{S}'(LR, i+1)$, starting from $\boldsymbol{S}'(LR, 1)$, can be established. It can be shown (see appendix C) that the matrix $\boldsymbol{S}'(LR, i+1)$ consists of four $M_C \times M_C$ blocks which are given by the following relations:

$$
\begin{aligned}
\boldsymbol{S}'_{11}(LR, i+1) &= [\mathbf{1} - \boldsymbol{T}_{11}^{-1}(i, i+1)\boldsymbol{S}'_{12}(LR, i)\boldsymbol{T}_{21}(i, i+1)]^{-1}\boldsymbol{T}_{11}^{-1}(i, i+1)\boldsymbol{S}'_{11}(LR, i) \\
\boldsymbol{S}'_{12}(LR, i+1) &= [\mathbf{1} - \boldsymbol{T}_{11}^{-1}(i, i+1)\boldsymbol{S}'_{12}(LR, i)\boldsymbol{T}_{21}(i, i+1)]^{-1} \\
&\quad \times [\boldsymbol{T}_{11}^{-1}(i, i+1)\boldsymbol{S}'_{12}(LR, i)\boldsymbol{T}_{22}(i, i+1) - \boldsymbol{T}_{11}^{-1}(i, i+1)\boldsymbol{T}_{12}(i, i+1)] \\
\boldsymbol{S}'_{21}(LR, i+1) &= \boldsymbol{S}'_{21}(LR, i) + \boldsymbol{S}'_{22}(LR, i)\boldsymbol{T}_{21}(i, i+1)\boldsymbol{S}'_{11}(LR, i+1) \\
\boldsymbol{S}'_{22}(LR, i+1) &= \boldsymbol{S}'_{22}(LR, i)\boldsymbol{T}_{21}(i, i+1)\boldsymbol{S}'_{12}(LR, i+1) + \boldsymbol{S}'_{22}(LR, i)\boldsymbol{T}_{22}(i, i+1),
\end{aligned}
\tag{21}
$$

in which $\boldsymbol{T}_{ij}(i, j) = \boldsymbol{T}_{ij}^{C}(i, j)$ was used for brevity. The final result, the total three-terminal scattering matrix for the system, $\boldsymbol{S}'(LR, N_C)$, may thus be obtained by iteratively using the above relation until $i + 1 = N_C$.

From the total scattering matrix, $\boldsymbol{S}'(LR, N_C)$, we can now calculate the transport properties of the device. The transmission and reflection coefficients between states in the various branches are easily obtained from $\boldsymbol{S}'(LR, N_C)$ by imposing the appropriate boundary conditions to the wavefunction. Consider for example an electron incident into the left branch of a Y-shaped three-terminal junction device in the transverse mode m with energy ε and wavevector $k_m^{L,1} = [2m^*(\varepsilon - E_m^{L,1})]^{1/2}$. The boundary condition for the wavefunction is

$$
\begin{pmatrix} \boldsymbol{A}^{R,1+} \\ \boldsymbol{A}^{L,1+} \\ \boldsymbol{A}^{C,N_C-} \end{pmatrix} = \begin{pmatrix} \mathbf{0} \\ \boldsymbol{I}_m \\ \mathbf{0} \end{pmatrix}
\tag{22}
$$

[1] From numerical calculations we found that in many cases, the matrices $\boldsymbol{F}^{L,R}$ are ill conditioned and hence give rise to numerical errors when inverted. Thus, in our approach the formalism was derived so as to avoid any inversions of $\boldsymbol{F}^{L,R}$.

where $\boldsymbol{I}_m$ is a column vector with elements given by $(\boldsymbol{I}_m)_n = \delta_{nm}$. Thus, equation (13) yields

$$\begin{pmatrix} \boldsymbol{A}^{C,N_C+} \\ \boldsymbol{A}^{R,1-} \\ \boldsymbol{A}^{L,1-} \end{pmatrix} = \begin{bmatrix} \boldsymbol{S}'_{CR}(LR,N_C) & \boldsymbol{S}'_{CL}(LR,N_C) & \boldsymbol{S}'_{CC}(LR,N_C) \\ \boldsymbol{S}'_{RR}(LR,N_C) & \boldsymbol{S}'_{RL}(LR,N_C) & \boldsymbol{S}'_{RC}(LR,N_C) \\ \boldsymbol{S}'_{LR}(LR,N_C) & \boldsymbol{S}'_{LL}(LR,N_C) & \boldsymbol{S}'_{LC}(LR,N_C) \end{bmatrix} \begin{pmatrix} \boldsymbol{0} \\ \boldsymbol{I}_m \\ \boldsymbol{0} \end{pmatrix} \tag{23}$$

in which we have written the full scattering matrix in block form, each block, $\boldsymbol{S}'_{bb'}$, having dimensions $M_b \times M_{b'}$ (where $b, b' = L, R, C$). Consequently, we can express the probability that an electron incident from the left branch in the transverse mode m will be transmitted or reflected into a transverse mode n of one of the three branches in terms of the scattering matrix of equation (23) according to

$$\begin{aligned} T_{CL}^{nm} &= \frac{k_n^C}{k_m^L}|(\boldsymbol{A}^{C,N_C+})_n|^2 = \frac{k_n^C}{k_m^L}|(\boldsymbol{S}'_{CL})_{nm}|^2 \\ T_{RL}^{nm} &= \frac{k_n^R}{k_m^L}|(\boldsymbol{A}^{R,1-})_n|^2 = \frac{k_n^R}{k_m^L}|(\boldsymbol{S}'_{RL})_{nm}|^2 \\ R_{LL}^{nm} &= \frac{k_n^L}{k_m^L}|(\boldsymbol{A}^{L,1-})_n|^2 = \frac{k_n^L}{k_m^L}|(\boldsymbol{S}'_{LL})_{nm}|^2, \end{aligned} \tag{24}$$

where the wavevectors k_n^b are real corresponding to propagating states. All transmission probabilities of the general form $T_{bb'}^{nm}$ may similarly be obtained by applying the corresponding boundary conditions and using the blocks $\boldsymbol{S}'_{bb'}$ of equation (23).

For a given energy ε, the total transmission between branches b and b' is obtained by summing over all states which can carry current in the two branches b and b' according to the relation

$$T_{b'b}(\varepsilon) = \sum_{n,m}^{(occ)} \frac{k_n^{b'}}{k_m^b}|(\boldsymbol{S}'_{b'b})_{nm}|^2, \tag{25}$$

where the summation is to be done over all states n and m which are occupied at the given energy. Similarly, the total reflection in branch b at energy ε may be obtained from

$$R_{bb}(\varepsilon) = \sum_{n,m}^{(occ)} \frac{k_n^b}{k_m^b}|(\boldsymbol{S}'_{bb})_{nm}|^2. \tag{26}$$

The calculated transmission and reflection can be used within the Landauer–Büttiker formalism [48] to calculate transport properties such as conductance, current etc.

Current conservation implies that in each branch the following relation should hold:

$$\sum_{b'(\neq b)} T_{b'b}(\varepsilon) + R_{bb}(\varepsilon) = M_b^p, \tag{27}$$

where M_b^p is the number of propagating modes in branch b. In numerical calculations, current conservation serves as an important criterion for the validity of the results and therefore a check of the relation (27) must be implemented accordingly.

3. Discussion and application to Y-shaped TBJs

The theoretical approach derived in the previous section provides a flexible tool for the study of electron transport through general Y-shaped three-terminal junctions which, in principle, can have any type of complicated geometry and/or potential profile. The longitudinal variations of the potential profile are inherently modelled by the division of the structure into segments

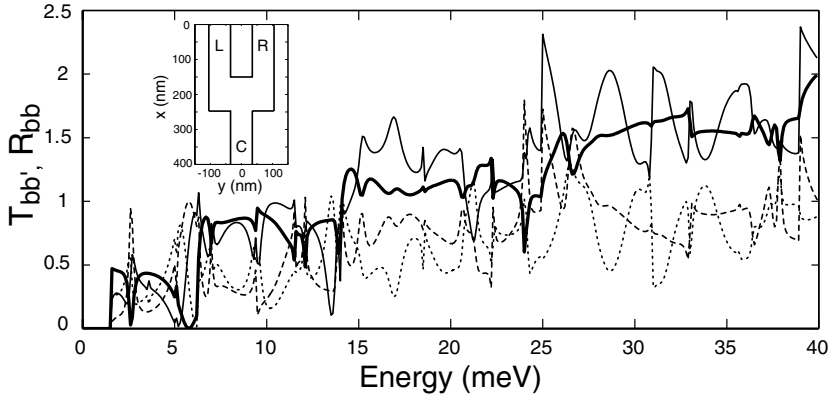

Figure 3. Transmission ($T_{bb'}$) and reflection (R_{bb}) through a symmetric Y-junction consisting of three 70 nm wide perfect leads, connected via a $210 \times 100\,\mathrm{nm}^2$ rectangular coupling window. The curves correspond to T_{LC} (thick curve), R_{LL} (thin curve), T_{LR} (dotted curve) and R_{CC} (dashed curve). All other transmission and reflections may be obtained from the symmetry of the system. The inset shows the geometry of the device.

which are small enough such that the potential in each segment is of transverse dependence only. An arbitrary transverse modulation of the potential profile may, however, also be included in the modelling, thus enabling the study of realistic two-dimensional potentials. An advantage of the method over theoretical approaches based on lattice models is that the method is less time consuming.

Another advantage of the formalism is the numerical stability. The use of the scattering-matrix method is advantageous due to the fact that evanescent states are fully included in the formalism (unlike the transfer-matrix method which becomes numerically unstable when calculating the properties of large structures with strong potential modulations) [37]. Also, our approach is formulated so as to avoid any inversions of the matrices $\boldsymbol{F}^{L(R)}$ which we found can give numerical instability in many cases (see footnote 1).

To illustrate the use of the formalism presented in this paper, we have calculated the transmission properties of a few Y-shaped junction structures with different geometries. In previous experiments on TBJs, waveguides [8, 9, 49] and quantum point contacts [10] were connected to coupling windows of sizes around 100 nm, the lithographic dimensions of the quantum point contacts and waveguides being of the same order. In the following we will show results for the transport characteristics of three, symmetric, Y-shaped TBJs with 70 nm wide waveguides, in which $U_s^{b,i}(y) = 0$.

In figure 3 we show the transmissions and reflections through an idealized symmetric Y-shaped TBJ in which three perfect 70 nm wide and infinitely long leads are connected by a $210 \times 100\,\mathrm{nm}^2$ rectangular coupling window (see the inset of figure 3). The confining potential in the device is of square-well type, thus the matrix elements of $U_c^{b,i}(y)$ in equations (6) are easily evaluated. The effective mass was set to $m^* = 0.047\,m_0$ corresponding to the InGaAs system.

The computation of the transport properties of such a device is very fast, since only a few segments are needed in the modelling of the structure, thus wavefunction matching and matrix handling are only performed at a handful of interfaces. Depending on the energy range studied, a transmission spectrum such as the one calculated in figure 3 may be obtained within minutes on a present day modern PC.

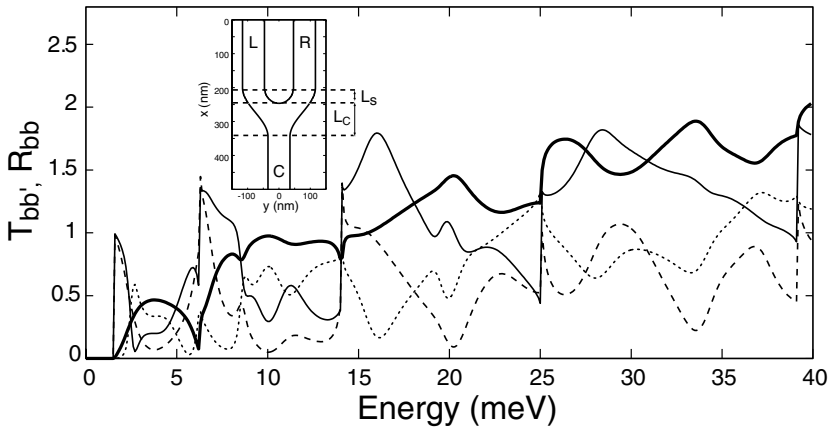

Figure 4. Transmissions ($T_{bb'}$) and reflections (R_{bb}) through a symmetric Y-junction consisting of three 70 nm wide perfect leads (the inset shows the geometry of the device). The three branches are connected via a coupling window of length $L_C = 100$ nm, the total transverse changes in the structure occurring over a length of 150 nm ($L_s = 50$ nm, $L_c = 100$ nm, see inset). The curves correspond to T_{LC} (thick curve), R_{LL} (thin curve), T_{LR} (dotted curve) and R_{CC} (dashed curve). All other transmissions and reflections may be obtained from the symmetry of the system.

Numerical results are shown in figure 3. The four different curves correspond to T_{LC} (thick curve), R_{LL} (thin curve), T_{LR} (dotted curve) and R_{CC} (dashed curve), the notation $T(R)_{bb'}$ denoting transmissions (T) and reflections (R) between branches b' and b. The remaining transmissions and reflections can be obtained from the curves in figure 3 due to the symmetry of the system. It is seen that the transmission and reflection between the various branches displays complex features, including peaks and dips of varying sharpness and amplitudes, which originate from the complicated density of states created in the coupling window in the central region of the device. Incoming electrons from the different branches experience strong scatterings and mode mixings, giving rise to the complex behaviour.

Structures studied in [8, 9, 49] where the waveguides and coupling window have smooth variations of the transverse widths along the direction of transport may also be easily modelled. Consider for example the structure in the inset of figure 4. Similarly to the structure studied in figure 3, the device is symmetric, containing three branches, each 70 nm wide. However, in this case we have generated a structure in which the lateral changes occur over 150 nm, such that it resembles typical structures used in the experiments. The central region is in this case 100 nm long similarly to the structure studied in figure 3. We still assume $U_s^{b,i}(y) = 0$ and $m^* = 0.047\ m_0$.

In the modelling of this structure we have assumed 400 segments for each of the left and right branches and 100 segments for the central branch, such that the segments in the regions of varying lateral confinement are of sub-nm sizes. This type of calculation is also easily performed with moderate computing facilities.

The calculated transmissions and reflections for the device are shown in figure 4. Again we display T_{LC} (thick curve), R_{LL} (thin curve), T_{LR} (dotted curve) and R_{CC} (dashed curve), and the rest of the transmissions and reflections can be found from these curves based on the symmetry of the system. Comparison between figures 3 and 4 shows that the smoothness introduced in the lateral confinement of the structure along the direction of transport eliminates many of the sharp features seen in figure 3. However, the transmission and reflection spectra still show strong fluctuations due to the formation of quasi-bound states in the central junction region.

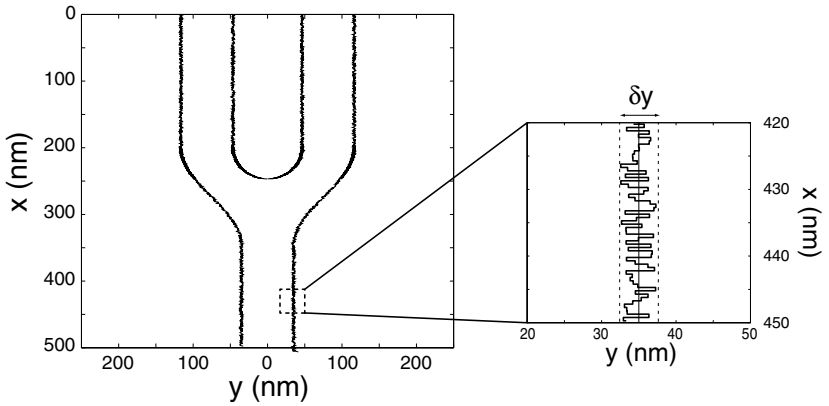

Figure 5. Example of a Y-junction device (with identical geometrical parameters to the structure studied in figure 4) with corrugated boundaries caused by, e.g., the process of etching. In this particular sample the amplitude, δy, of the boundary roughness was set to $\delta y = 5$ nm.

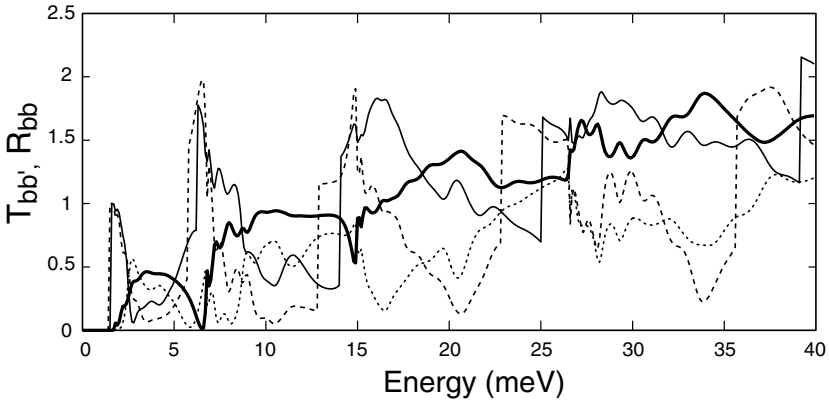

Figure 6. Transmission ($T_{bb'}$) and reflection (R_{bb}) as a function of energy for the Y-junction device as shown in figure 5. The curves correspond to T_{LC} (thick curve), R_{LL} (thin curve), T_{LR} (dotted curve) and R_{CC} (dashed curve). All other transmission and reflections may be obtained from the symmetry of the system.

Even more realistic model structures with the presence of, for instance, impurity scattering and/or boundary roughness scattering [$U_s^{b,i}(y) \neq 0$] may also be studied without drastically increasing the computational time. The latter may for instance occur in experiments due to the process of etching. The boundary roughness may be modelled, e.g., as in figure 5 where we show the geometry of a Y-junction structure with identical geometrical parameters to the structure studied in figure 4. However, as shown in the figure, the boundaries are corrugated, such that the transverse positions of the boundaries fluctuate within an interval δy, which in this particular case is chosen as $\delta y = 5$ nm.

The transmissions and reflections through the structure of figure 5 are shown in figure 6, where each of the curves has the same meaning as in figures 3 and 4, i.e., the thick curve for T_{LC}, the thin curve for R_{LL}, the dotted curve for T_{LR} and the dashed curve for R_{CC}. It is seen by comparison with figure 4 that the presence of boundary roughness in the system gives rise to new fluctuations in the transmission and reflection spectra.

4. Summary and remarks

In summary, in this paper we have derived a formalism based on the scattering-matrix method for the calculation of electron transport through three-terminal junctions. We have shown how the method may be implemented for the modelling of general Y-junctions with complicated geometries and potential profiles and have illustrated the use of the method by calculating the transmission properties of a few model Y-shaped TBJ structures with geometrical parameters typical to experiments. Complicated transport characteristics are shown to occur in Y-shaped TBJ structures, which are due to complex scatterings between the three incoming leads and the central connecting region. The flexibility of the method, arising from the use of a common basis approach, allows for the study of the effects of various scatterings such as boundary roughness and impurity scatterings, as well as the modelling of arbitrary shapes of the device. The formalism presented in this paper is a useful tool for extensive studies of the properties of TBJs, which recently have received attention due to their potential use as building blocks in future nanoscale electronic devices.

Before closing, we would like to note that it is interesting to study the nonlocal effect of electron transport and to calculate the multi-terminal resistance of various Y-junction devices with and without an applied magnetic field, based on the transmissions obtained with the present formalism. The nonlocal electron transport in multi-terminal systems has been subjected to an extensive study in recent years [21, 50–53] and a few interesting devices, such as the Hall magnetometer [52] and the Hall potentiometer [53], have been proposed based on these studies. It should also be noted that the formulation presented in this work does not include the effects of interaction. There has been much interest in the search for unconventional electron behaviour, such as the Luttinger-liquid behaviour [54], deviating from the single-particle picture. The evidence for the existence of the Luttinger-liquid behaviour in one-dimensional quantum wires [55] and carbon nanotubes [56, 57] has been previously reported. The question of whether this behaviour can be observable in a Y-junction waveguide or carbon nanotube structure is certainly interesting to study. However, such a study is beyond the scope of the present work.

Acknowledgments

This work was supported by the Swedish Foundation for Strategic Research (SSF) and the Swedish Research Council (VR) and by the European Commission through the Information Society Technologies (IST) programme project NEAR. Furthermore, the authors gratefully acknowledge Xue-Hua Wang for fruitful discussions and for critical reading of the manuscript.

Appendix A. Evaluation of $\boldsymbol{S^L(1,2)}$ and $\boldsymbol{S^R(1,2)}$

The scattering matrices $\boldsymbol{S}^L(1,2)$ and $\boldsymbol{S}^R(1,2)$ which connect the amplitudes of the first and second segments of the left and right branches are obtained from

$$\begin{aligned}
\boldsymbol{S}^b_{11}(1,2) &= [\boldsymbol{T}^b_{11}(1,2)]^{-1} \\
\boldsymbol{S}^b_{12}(1,2) &= -[\boldsymbol{T}^b_{11}(1,2)]^{-1}\boldsymbol{T}^b_{12}(1,2) \\
\boldsymbol{S}^b_{21}(1,2) &= \boldsymbol{T}^b_{21}(1,2)[\boldsymbol{T}^b_{11}(1,2)]^{-1} \\
\boldsymbol{S}^b_{22}(1,2) &= -\boldsymbol{T}^b_{21}(1,2)[\boldsymbol{T}^b_{11}(1,2)]^{-1}\boldsymbol{T}^b_{12}(1,2) + \boldsymbol{T}^b_{22}(1,2),
\end{aligned} \tag{A.1}$$

where $\boldsymbol{T}^b(1,2)$ is given by equation (10) with $x_0^{b,1} = x_0^{b,2}$. For derivation see Xu [37].

Appendix B. Derivation of $S'(LR, 1)$

In the following we will give a short derivation of the scattering matrix $S'(LR, 1)$. Using the definitions made in equation (20) we can write the relation (15) according to

$$\begin{pmatrix} P & P \\ Q & -Q \end{pmatrix} \begin{pmatrix} \Gamma & 0 \\ 0 & \Gamma^{-1} \end{pmatrix} \begin{pmatrix} A^{R,N_R+} \\ A^{L,N_L+} \\ A^{R,N_R-} \\ A^{L,N_L-} \end{pmatrix} = \begin{pmatrix} D^{C,1} & D^{C,1} \\ R & -R \end{pmatrix} \begin{pmatrix} A^{C,1+} \\ A^{C,1-} \end{pmatrix}. \tag{B.1}$$

After some elementary matrix algebra one can show that

$$\begin{pmatrix} A^{R,N_R-} \\ A^{L,N_L-} \end{pmatrix} = \Gamma W \Gamma \begin{pmatrix} A^{R,N_R+} \\ A^{L,N_L+} \end{pmatrix} + 2\Gamma U^{-1} Q^{-1} R A^{C,1-} \tag{B.2}$$

(in which care must be taken as to avoid any inversions of the matrices, $F^{L,R}$ (see footnote 1)). Using equations (12) and (B.2) one can show that

$$\begin{aligned} \begin{pmatrix} A^{R,1-} \\ A^{L,1-} \end{pmatrix} &= \{S_{21} + S_{22}[1 - \Gamma W \Gamma S_{12}]^{-1}[\Gamma W \Gamma S_{11}]\} \begin{pmatrix} A^{R,1+} \\ A^{L,1+} \end{pmatrix} \\ &\quad + 2S_{22}[1 - \Gamma W \Gamma S_{12}]^{-1} \Gamma U^{-1} Q^{-1} R A^{C,1-}, \end{aligned} \tag{B.3}$$

where the blocks S_{ij} are given in equation (20).

Since the three-terminal scattering matrix $S'(LR, 1)$ relates the amplitudes $A^{C,1+}$, $A^{R,1-}$, $A^{L,1-}$ to the amplitudes $A^{R,1+}$, $A^{L,1+}$, $A^{C,1-}$ we now need to find a relevant expression for $A^{C,1+}$. From equation (B.1) one can show that

$$2(D^{C,1})^{-1} P \Gamma \begin{pmatrix} A^{R,N_R+} \\ A^{L,N_L+} \end{pmatrix} = [1 + (D^{C,1})^{-1} P Q^{-1} R] A^{C,1+} + [1 - (D^{C,1})^{-1} P Q^{-1} R] A^{C,1-}. \tag{B.4}$$

Equation (12) is again used in order to express the amplitudes A^{b,N_b+} in terms of $A^{b,1\pm}$. Together with the relation (B.2), equation (B.4) may be rewritten as

$$\begin{aligned} A^{C,1+} &= 2[1 + (D^{C,1})^{-1} P Q^{-1} R]^{-1} (D^{C,1})^{-1} P \Gamma [1 - S_{12} \Gamma W \Gamma]^{-1} S_{11} \begin{pmatrix} A^{R,1+} \\ A^{L,1+} \end{pmatrix} \\ &\quad + [1 + (D^{C,1})^{-1} P Q^{-1} R]^{-1} \{4(D^{C,1})^{-1} P \Gamma [1 - S_{12} \Gamma W \Gamma]^{-1} \\ &\quad \times S_{12} \Gamma U^{-1} Q^{-1} R - 1 + (D^{C,1})^{-1} P Q^{-1} R\} A^{C,1-}. \end{aligned} \tag{B.5}$$

The blocks of $S'(LR, 1)$ (equation (19)) are then readily obtained from (B.3) and (B.5).

Appendix C. Iterative relation for $S'(LR, i + 1)$

Knowing $S'(LR, 1)$ it is now possible to calculate the total scattering matrix for the system using an iterative approach. Assume for instance that the scattering matrix $S'(LR, i)$ is known and thus

$$\begin{pmatrix} A^{C,i+} \\ A^{R,1-} \\ A^{L,1-} \end{pmatrix} = \begin{pmatrix} S'_{11}(LR, i) & S'_{12}(LR, i) \\ S'_{21}(LR, i) & S'_{22}(LR, i) \end{pmatrix} \begin{pmatrix} A^{R,1+} \\ A^{L,1+} \\ A^{C,i-} \end{pmatrix}. \tag{C.1}$$

The amplitudes of the states in two adjacent segments i and $j = i + 1$ in the central branch may be related by a transfer matrix $T^C(i, j = i + 1)$

$$\begin{pmatrix} A^{C,j+} \\ A^{C,j-} \end{pmatrix} = \begin{pmatrix} T^C_{11}(i, j) & T^C_{12}(i, j) \\ T^C_{21}(i, j) & T^C_{22}(i, j) \end{pmatrix} \begin{pmatrix} A^{C,i+} \\ A^{C,i-} \end{pmatrix}, \tag{C.2}$$

where $\boldsymbol{T}^C$ is given by equation (10). By eliminating $\boldsymbol{A}^{C,i\pm}$ from the above two equations we can show that

$$\begin{aligned}\boldsymbol{A}^{C,j+} &= [\mathbf{1} - \boldsymbol{T}_{11}^{-1}(i,j)\boldsymbol{S}'_{12}(LR,i)\boldsymbol{T}_{21}(i,j)]^{-1}\boldsymbol{T}_{11}^{-1}(i,j)\boldsymbol{S}'_{11}(LR,i)\begin{pmatrix}\boldsymbol{A}^{R,1+}\\ \boldsymbol{A}^{L,1+}\end{pmatrix} \\ &\quad + [\mathbf{1} - \boldsymbol{T}_{11}^{-1}(i,j)\boldsymbol{S}'_{12}(LR,i)\boldsymbol{T}_{21}(i,j)]^{-1} \\ &\quad \times [\boldsymbol{T}_{11}^{-1}(i,j)\boldsymbol{S}'_{12}(LR,i)\boldsymbol{T}_{22}(i,j) - \boldsymbol{T}_{11}^{-1}(i,j)\boldsymbol{T}_{12}(i,j)]\boldsymbol{A}^{C,j-} \\ \begin{pmatrix}\boldsymbol{A}^{R,1-}\\ \boldsymbol{A}^{L,1-}\end{pmatrix} &= [\boldsymbol{S}'_{21}(LR,i) + \boldsymbol{S}'_{22}(LR,i)\boldsymbol{T}_{21}(i,j)\boldsymbol{S}'_{11}(LR,j)]\begin{pmatrix}\boldsymbol{A}^{R,1+}\\ \boldsymbol{A}^{L,1+}\end{pmatrix} \\ &\quad + [\boldsymbol{S}'_{22}(LR,i)\boldsymbol{T}_{21}(i,j)\boldsymbol{S}'_{12}(LR,j) + \boldsymbol{S}'_{22}(LR,i)\boldsymbol{T}_{22}(i,j)]\boldsymbol{A}^{C,j-}, \qquad \text{(C.3)}\end{aligned}$$

from which the blocks $\boldsymbol{S}'_{ij}(LR,j)$ of equation (21) can be obtained.

References

[1] Ijima S 1991 *Nature* **354** 56
[2] Qin L C, Zhao X, Hirahara K, Miyamoto Y, Ando Y and Iijima S 2000 *Nature* **408** 50
[3] Wang N, Tang Z K, Li G D and Chen J S 2000 *Nature* **408** 50
[4] Li J, Papadopoulos C and Xu J 1999 *Nature* **402** 254
[5] Papadopoulos C, Rakitin A, Li J, Vedeneev A S and Xu J M 2000 *Phys. Rev. Lett.* **85** 3476
[6] Satishkumar B C, Thomas P J, Govindaraj A and Rao C N R 2000 *Appl. Phys. Lett.* **77** 2530
[7] Li W Z, Wen J G and Ren Z F 2001 *Appl. Phys. Lett.* **79** 1879
[8] Hieke K and Ulfward M 2000 *Phys. Rev.* B **62** 16727
[9] Worschech L, Xu H Q, Forchel A and Samuelson L 2001 *Appl. Phys. Lett.* **79** 3287
[10] Shorubalko I, Xu H Q, Maximov I, Omling P, Samuelson L and Seifert W 2001 *Appl. Phys. Lett.* **79** 1384
[11] Shorubalko I, Xu H Q, Maximov I, Nilsson D, Omling P, Samuelson L and Seifert W 2002 *IEEE Electron Device Lett.* **23** 377
[12] Palm T and Thylén L 1992 *Appl. Phys. Lett.* **60** 237
[13] Palm T 1995 *Phys. Rev.* B **52** 13773
[14] Palm T 1995 *Phys. Rev.* B **52** 11 284
[15] Xu H Q 2001 *Appl. Phys. Lett.* **78** 2064
[16] Xu H Q 2002 *Appl. Phys. Lett.* **80** 853
[17] Andriotis A N, Menon M, Srivastava D and Chernozatonskii L 2001 *Appl. Phys. Lett.* **79** 266
[18] Andriotis A N, Menon M, Srivastava D and Chernozatonskii L 2001 *Phys. Rev. Lett.* **87** 066802
[19] Xu H Q 2002 *Physica* E **13** 942
[20] Maximov I, Carlberg P, Wallin D, Shorubalko I, Seifert W, Xu H Q, Montelius L and Samuelson L 2002 *Nanotechnology* **13** 666
[21] Beenakker C W J and van Houten H 1991 *Solid State Physics: Advances in Research and Applications* vol 44, ed H Ehrenreich and D Turnbull (San Diego, CA: Academic) p 1
[22] Exner P and Seba P 1989 *J. Math. Phys.* **30** 2574
[23] Xu H Q 1993 *Phys. Rev.* B **47** 9537
[24] Kawamura T and Leburton J P 1993 *Phys. Rev.* B **48** 8857
[25] Pavlov B S, Popov I Y and Frolov S V 2002 *Eur. Phys. J.* B **21** 283
[26] Yuan S and Gu B 1993 *Z. Phys.* B **92** 47
[27] Kasai H, Mitsutake K and Okiji A 1991 *J. Phys. Soc. Japan* **60** 1679
Ishio H and Nakamura K 1992 *J. Phys. Soc. Japan* **61** 2649
[28] Linke H, Sheng W, Löfgren A, Xu H Q, Omling P and Lindelof P E 1998 *Europhys. Lett.* **44** 341
[29] Xu H Q and Sheng W 1998 *Phys. Rev.* B **57** 11903
[30] Tamura H and Ando T 1991 *Phys. Rev.* B **44** 1792
[31] Csontos D and Xu H Q 2000 *Appl. Phys. Lett.* **77** 2364
[32] Nakazato K and Blaikie R J 1991 *J. Phys.: Condens. Matter* **3** 5729
[33] Wu H, Sprung D W L and Martorell J 1992 *Phys. Rev.* B **45** 11960
[34] Stratford K and Beeby J L 1993 *J. Phys.: Condens. Matter* **5** L289
[35] Baranger H U, DiVicenzo D P, Jalabert R A and Stone A D 1991 *Phys. Rev.* B **44** 10637
[36] Sols F, Macucci M, Ravaioli U and Hess K 1989 *J. Appl. Phys.* **66** 3892
[37] Xu H Q 1994 *Phys. Rev.* B **50** 8469

[38] Xu H Q 1995 *Phys. Rev.* B **52** 5803
[39] Cahay M, Bandyopadhyay S and Frohne H R 1990 *J. Vac. Sci. Technol.* B **8** 1399
[40] Ko D Y K and Inkson J C 1988 *Phys. Rev.* B **38** 9945
[41] Mizuta H 1999 *Microelectron. J.* **30** 1007
[42] Csontos D and Xu H Q 2001 *Japan. J. Appl. Phys.* **40** 1966
[43] Sheng W 2001 *J. Phys.: Condens. Matter* **13** 1247
[44] Sheng W 1997 *J. Appl. Phys.* **81** 6210
[45] Sheng W and Xu H Q 1998 *J. Appl. Phys.* **84** 2146
[46] Sheng W 1997 *J. Phys.: Condens. Matter* **9** 8369
[47] Xu H Q, Ji Z-L and Berggren K-F 1992 *Superlatt. Microstruct.* **12** 237
[48] Büttiker M 1986 *Phys. Rev. Lett.* **57** 1761
Büttiker M, Imry Y, Landauer R and Pinhas S 1985 *Phys. Rev.* B **31** 6207
[49] Worschech L, Weidner B, Reitzenstein S and Forchel A 2001 *Appl. Phys. Lett.* **78** 3325
[50] Takagaki Y and Ploog K 1996 *Phys. Rev.* B **53** 3885
[51] Thornton T J 1998 *Superlatt. Microstruct.* **23** 601
[52] Peeters F M and Li X Q 1998 *Appl. Phys. Lett.* **72** 572
[53] Baelus B J and Peeters F M 1999 *Appl. Phys. Lett.* **74** 1600
[54] Haldane F D M 1981 *J. Phys. C: Solid State Phys.* **14** 2585
Apel W and Rice T M 1982 *Phys. Rev.* B **26** 7063
Kane C L and Fisher M P A 1992 *Phys. Rev. Lett.* **68** 1220
Yue D, Glazman L I and Matveev 1994 *Phys. Rev.* B **49** 1966
Oreg Y and Finkel'stein A M 1996 *Phys. Rev.* B **54** R14265
Egger R and Gogolin A O 1997 *Phys. Rev. Lett.* **79** 5082
Kane C, Balents L and Fisher M P A 1997 *Phys. Rev. Lett.* **79** 5086
Bellucci S and González J 2001 *Phys. Rev.* B **64** 201106(R)
[55] Auslaender O M, Yacoby A, de Picciotto R, Baldwin K W, Pfeiffer L N and West K W 2000 *Phys. Rev. Lett.* **84** 1764
[56] Bochrath M, Cobden D H, Lu J, Rinzler A G, Smalley R E, Balents L and McEuen P L 1999 *Nature* **397** 598
[57] Graugnard E, de Pablo P J, Walsh B, Ghosh A W, Datta S and Reifenberger R 2001 *Phys. Rev.* B **64** 125407